Supplementary Table 1. Primer sequences for qRT-PCR (5'-3')

Gene	Forward	Reverse
PPA1	GCAGACAAGGATGTGTTCCA	GCAATGACCTTCCAGTCGGT
AP2	AAAGAAGTGGGAGTGGGCTT	CTCTTGTGGAAGTCACGCCT
PPARγ	CACAATGCCATCAGGTTTGG	GCTGGTCGATATCACTGGAGATC
Adiponectin	GTTCCCAATGTACCCATTCGC	TGTTGCAGTAGAACTTGCCAG
PGC1α	TATGGAGTGACATAGAGTGTGCT	CCACTTCAATCCACCCAGAAAG
Arpppo	GAAACTGCTGCCTCACATCCG	GCTGGCACAGTGACCTCACACG
PPA2	TTCTTCAAGCATGTAGCTGGTC	GGCTCCTCTGTGGCAATC
Nurf38	GGTTGGTCGCTTGTCC	TACCCTTCTTGATGTCCTG

Supplementary Table 2. Primer sequences for genotyping PCR (5'-3')

PPA1-deletion	CCACGCATTAAAGGCACGGC	TCGAATGTGTGGAGGGAGCG

Supplementary Table 3. Antibodies for western blot assays and reagents used in the experiment

Name	Source	Manufacturer	Catalog	Dilution
PPA1	Rabbit	Abcam, Cambridge, UK	ab96099	1:1000
CEBPα	Rabbit	Abcam, Cambridge, UK	ab40764	1:1000
beta Actin	Rabbit	Abcam, Cambridge, UK	ab8227	1:1000
PGC1α	Rabbit	Abcam, Cambridge, UK	ab72230	1:1000
OXPHOS Cocktail	Rabbit	Abcam, Cambridge, UK	ab110413	1:1000
AP2	Rabbit	Cell Signaling Technology, Danvers, MA, USA	#2120	1:1000
Ser473-phosphorylated Akt	Rabbit	Cell Signaling Technology, Danvers, MA, USA	#4060	1:1000
total Akt	Rabbit	Cell Signaling Technology, Danvers, MA, USA	#4691	1:1000
Opa1	Rabbit	Cell Signaling Technology, Danvers, MA, USA	#80471	1:1000
Mfn1	Rabbit	Cell Signaling Technology, Danvers, MA, USA	#14739	1:1000
Mfn2	Rabbit	Cell Signaling Technology, Danvers, MA, USA	#11925	1:1000
Phospho-Drp1(Ser616)	Rabbit	Cell Signaling Technology, Danvers, MA, USA	#4494	1:1000
Drp1	Rabbit	Cell Signaling Technology, Danvers, MA, USA	#8570	1:1000
Tom20	Rabbit	Cell Signaling Technology, Danvers, MA, USA	#42406	1:1000
Bcl-xL	Rabbit	Cell Signaling Technology, Danvers, MA, USA	#2764	1:1000
Cleaved PARP	Rabbit	Cell Signaling Technology, Danvers, MA, USA	#5625	1:1000
PARP	Rabbit	Cell Signaling Technology, Danvers, MA, USA	#9532	1:1000
Caspase-3	Rabbit	Cell Signaling Technology, Danvers, MA, USA	#9662	1:1000
α-tubulin	mouse	Cell Signaling Technology, Danvers, MA, USA	#2148	1:5000
PPAR-γ	Rabbit	Santa Cruz Biotechnology, Santa Cruz, CA, USA	sc-7196x	1:1000

GAPDH	Mouse	Bioworld Technology, Nanjing, China	MB001	1:5000
MitoTracker Red CMXRos		Invitrogen	M7512	1:1000
Hoechst 33342		Solarbio	B8040	1:1000

Supplementary Materials:

Non-targeted Metabolomic by LC-MS

Sample preparation

Cells were trypsin digested and centrifuged in the EP tubes and resuspended with prechilled 80% methanol and 0.1% formic acid by well vortex. Then the samples were melted on ice and whirled for 30 s. After the sonification for 6 min, they were centrifuged at 5,000 rpm, 4°C for 1 min. The supernatant was freeze-dried and dissolved with 10% methanol. Finally, the solution was injected into the LC-MS/MS system analysis.

UHPLC-MS/MS Analysis

UHPLC-MS/MS analyses were performed using a Vanquish UHPLC system (Thermo Fisher, Germany) coupled with an Orbitrap Q ExactiveTM HF-X mass spectrometer (Thermo Fisher, Germany) in Novogene Co., Ltd. (Beijing, China). Samples were injected onto a Hypesil Gold column (100×2.1 mm, 1.9 μm) using a 17-min linear gradient at a flow rate of 0.2 mL/min. The eluents for the positive polarity mode were eluent A (0.1% FA in Water) and eluent B (Methanol). The eluents for the negative polarity mode were eluent A (5 mM ammonium acetate, pH 9.0) and eluent B (Methanol). The solvent gradient was set as follows: 2% B, 1.5 min; 2-100% B, 12.0 min; 100% B, 14.0 min；100-2% B, 14.1 min；2% B, 17 min. Q ExactiveTM HF-X mass spectrometer was operated in positive/negative polarity mode with spray voltage

of 3.2 kV, capillary temperature of 320°C, sheath gas flow rate of 40 arb and aux gas flow rate of 10 arb.

Data processing and metabolite identification

The raw data files generated by UHPLC-MS/MS were processed using the Compound Discoverer 3.1 (CD3.1, Thermo Fisher) to perform peak alignment, peak picking, and quantitation for each metabolite. The main parameters were set as follows: retention time tolerance, 0.2 min; actual mass tolerance, 5 ppm; signal intensity tolerance, 30%; signal/noise ratio, 3; and minimum intensity, 100,000. After that, peak intensities were normalized to the total spectral intensity. The normalized data was used to predict the molecular formula based on additive ions, molecular ion peaks and fragment ions. And then peaks were matched with the mzCloud (https://www.mzcloud.org/), mzVaultand and MassList database to obtain the accurate qualitative and relative quantitative results. Statistical analyses were performed using the statistical software R (R version R-3.4.3), Python (Python 2.7.6 version) and CentOS (CentOS release 6.6), When data were not normally distributed, normal transformations were attempted using of area normalization method.

Data analysis

These metabolites were annotated using the KEGG database (https://www.genome.jp/kegg/pathway.html), HMDB database (https://hmdb.ca/metabolites) and LIPIDMaps database (http://www.lipidmaps.org/).

Principal components analysis (PCA) and Partial least squares discriminant analysis (PLS-DA) were performed at metaX (a flexible and comprehensive software for processing metabolomics data). We applied univariate analysis (t-test) to calculate the statistical significance (P-value). The metabolites with VIP > 1 and P-value < 0.05 and fold change $\geqslant$ 2 or FC $\leqslant$ 0.5 were considered to be differential metabolites. Volcano plots were used to filter metabolites of interest which based on log2 (Fold Change) and log10 (p-value) of metabolites.

For clustering heat maps, the data were normalized using z-scores of the intensity areas of differential metabolites and were plotted by Pheatmap package in R language. The correlation between differential metabolites were analyzed by cor() in R language (method=pearson). Statistically significant of correlation between differential metabolites were calculated by cor.mtest() in R language. P-value < 0.05 was considered as statistically significant and correlation plots were plotted by corrplot package in R language. The functions of these metabolites and metabolic pathways were studied using the KEGG database. The metabolic pathways enrichment of differential metabolites was performed, when ratio was satisfied by x/n > y/N, metabolic pathway was considered as enrichment, when P-value of metabolic pathway < 0.05, metabolic pathway was considered as statistically significant enrichment.

Supplementary Figures:

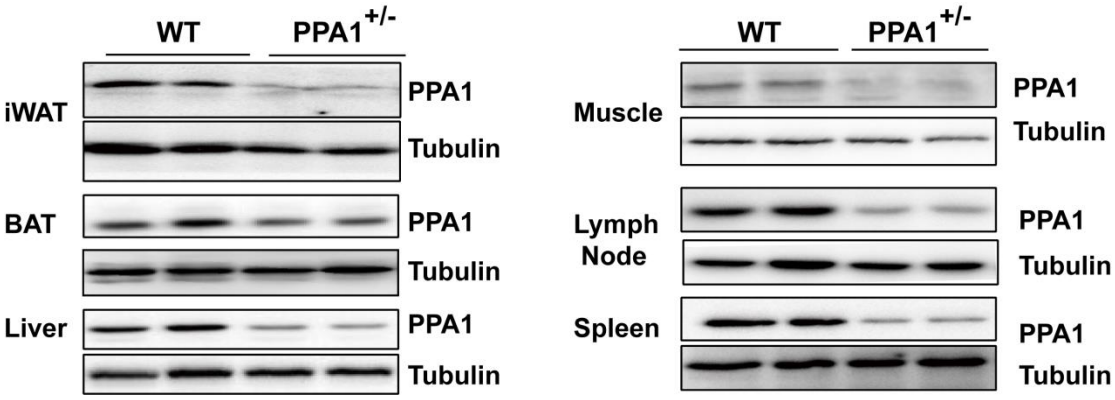

Supplementary Figure 1 The expression of PPA1 in different tissues of PPA1$^{+/-}$ mice was detected by Western Blot.

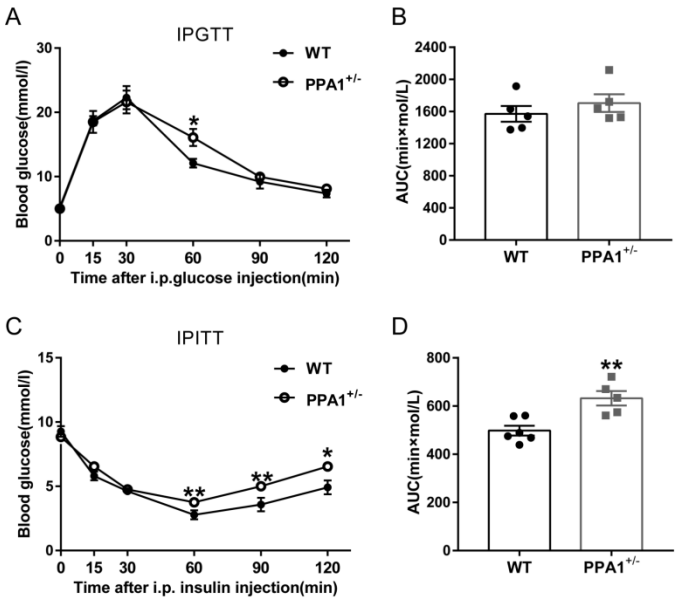

Supplementary Figure 2. Four-week-old female WT and PPA1$^{+/-}$ mice were subjected to a HFD for 12 weeks, GTT (A) and ITT (C) was performed and the area under curve was calculated (B,D). Data are represented as mean±SEM. *p<0.05, **p<0.01 compared with WT mice.

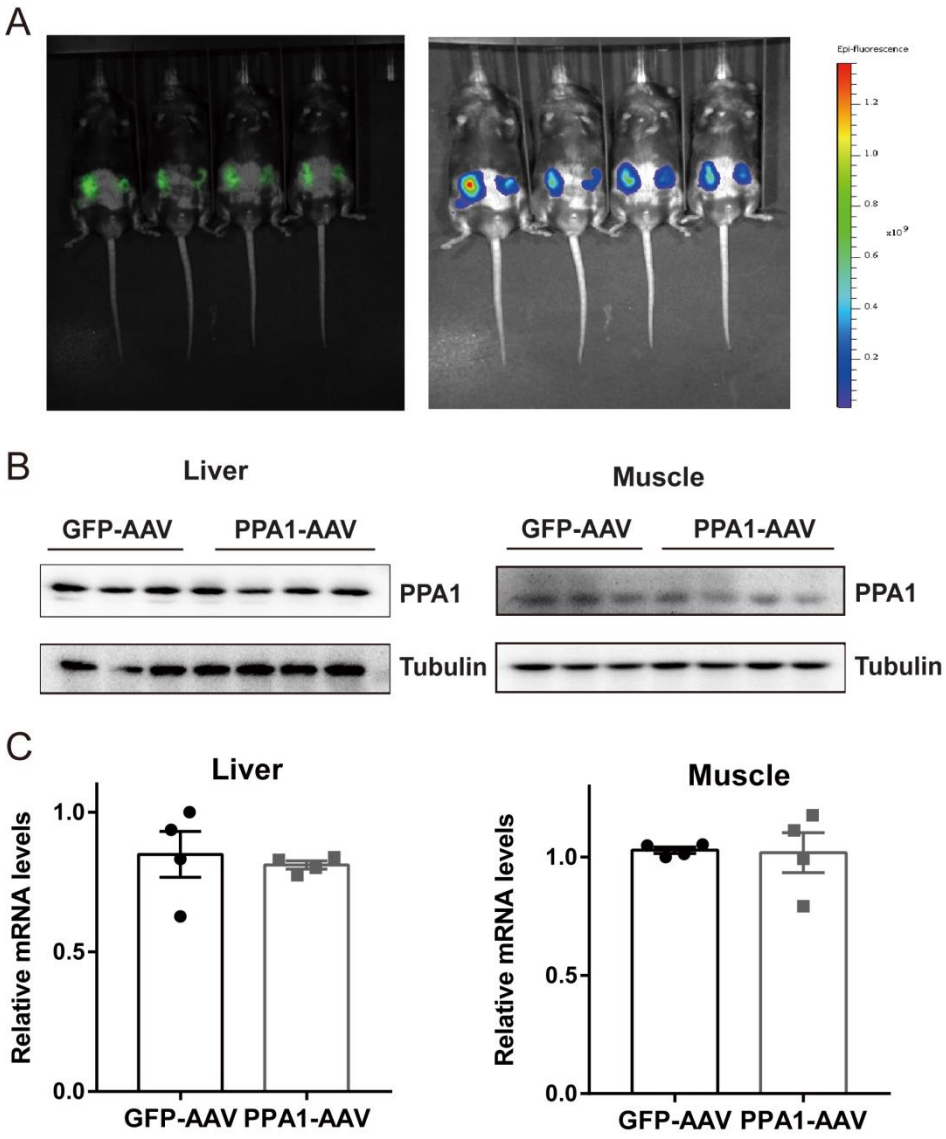

Supplementary Figure 3. Male 4-week-old PPA1$^{+/-}$ mice were injected with GFP-AAV or PPA1-AAV in inguinal fat (1×10^{12} v.g/ml, in a total volume of 30 μl). Two weeks later, these mice were fed with HFD for 12 weeks. A. Mice were subjected to visible light monitoring using the Visible light 3D imaging system. Representive photographic image of the animal under white light and a quantitative fluorescent signal via the Spectrum IVIS system (Brucker). B,C. Expression of PPA1 in liver and muscle was detected by Western Blot (B) and Q-PCR (C).

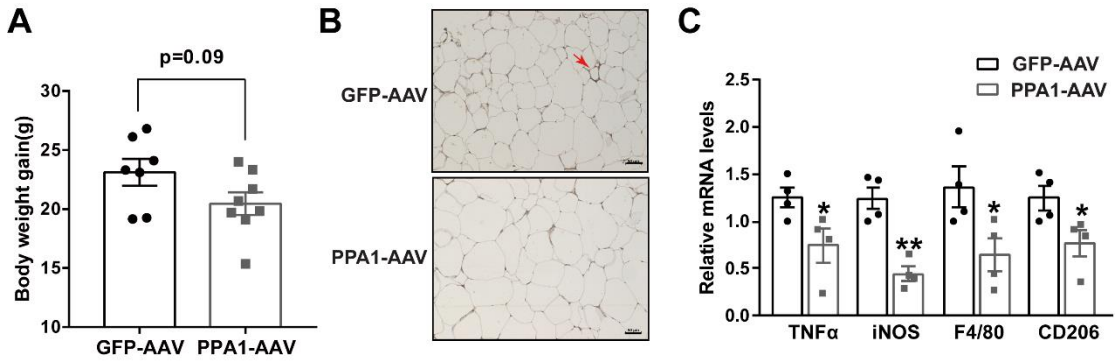

Supplementary Figure 4. PPA1$^{+/-}$ mice injected with GFP-AAV or PPA1-AAV in inguinal fat (1×10^{12} v.g/ml, in a total volume of 30 μl). Two weeks later, these mice were fed with HFD for 12 weeks. A. The body weight gain was detected. B. F4/80 immunostaining in iWAT with arrows indicating crown-like structures. Scale Bar=50 μm. C. Relative mRNA levels of inflammatory factors in iWAT from GFP-AAV and PPA1-AAV mice. *p<0.05, **p<0.01 compared with GFP-AAV mice.

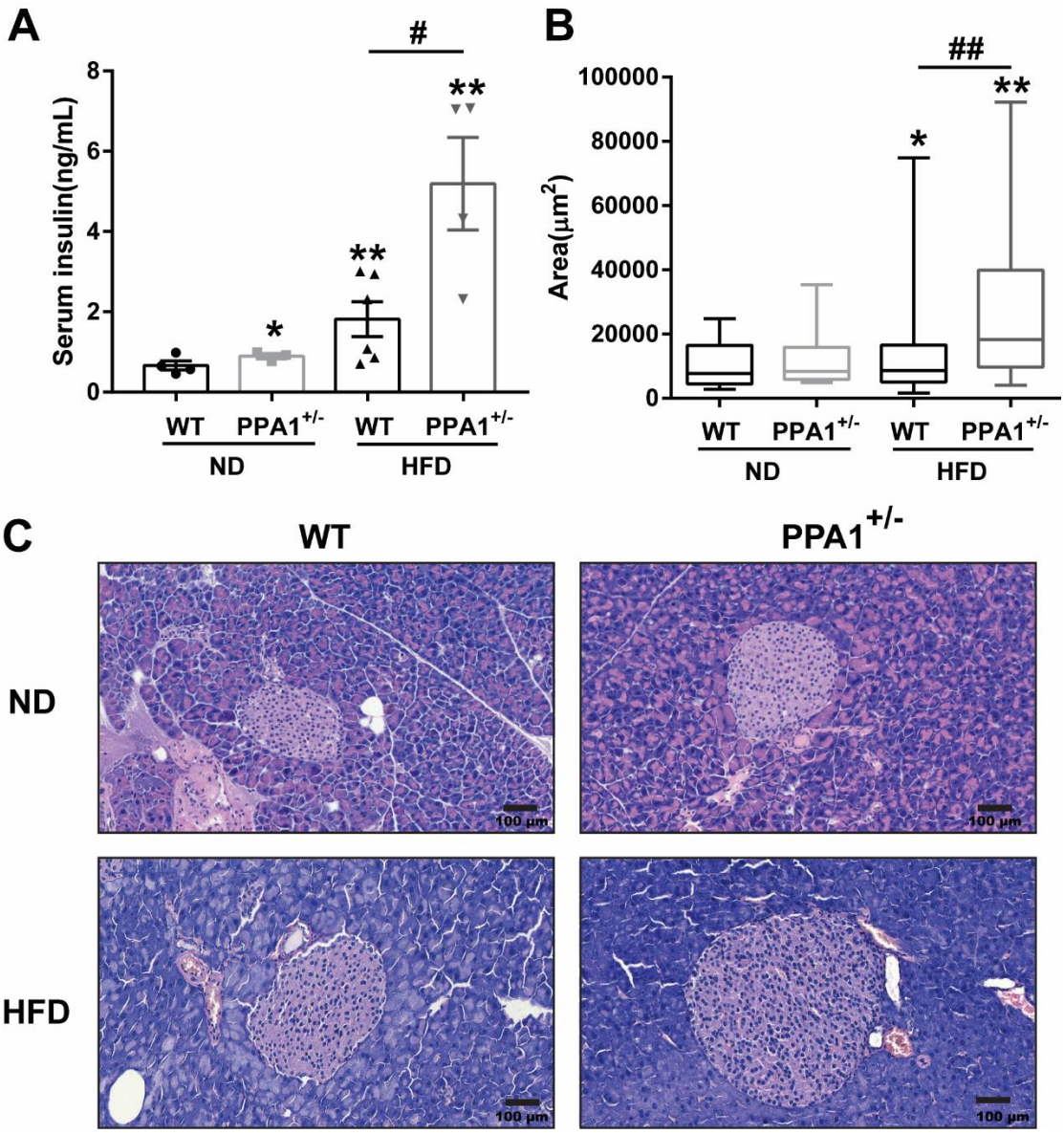

Supplementary Figure 5. Compensatory expansion of pancreatic islets was observed in PPA1$^{+/-}$ mice (n=6). A: Plasma insulin level in WT and PPA1$^{+/-}$ mice either with or without HFD-feeding; B: Islet area was analyzed; C: Representative images of H&E staining of pancreatic sections. Data are represented as mean±SEM. *p<0.05, **p<0.01 compared with NCD WT mice. #p<0.05, ##p<0.01 compared with HFD WT mice.

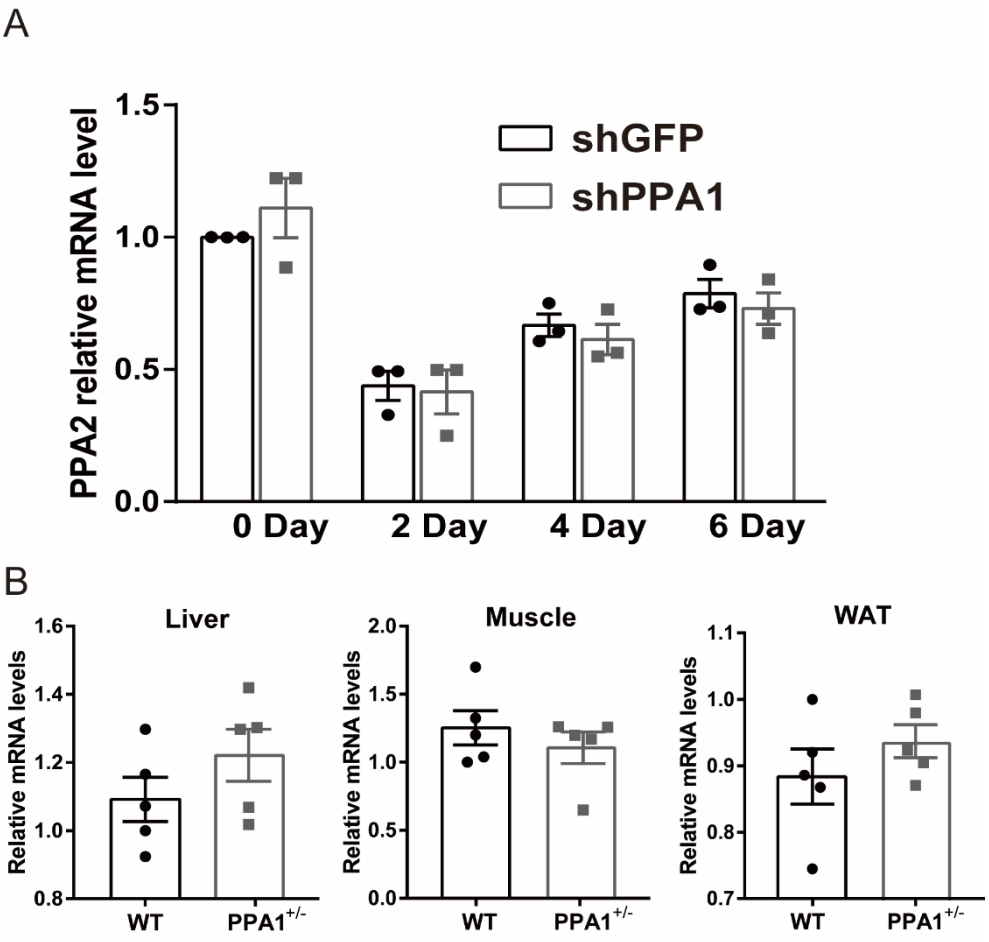

Supplementary Figure 6. Expression of PPA2 was detected both *in vitro* and *in vivo*. A. 3T3-L1 cells were transduced with shGFP or shPPA1 and collected at indicated time points post induction. Expression of PPA2 was detected by Q-PCR. B. Expression of PPA2 was detected in liver, muscle and WAT from WT and $PPA1^{+/-}$ mice.

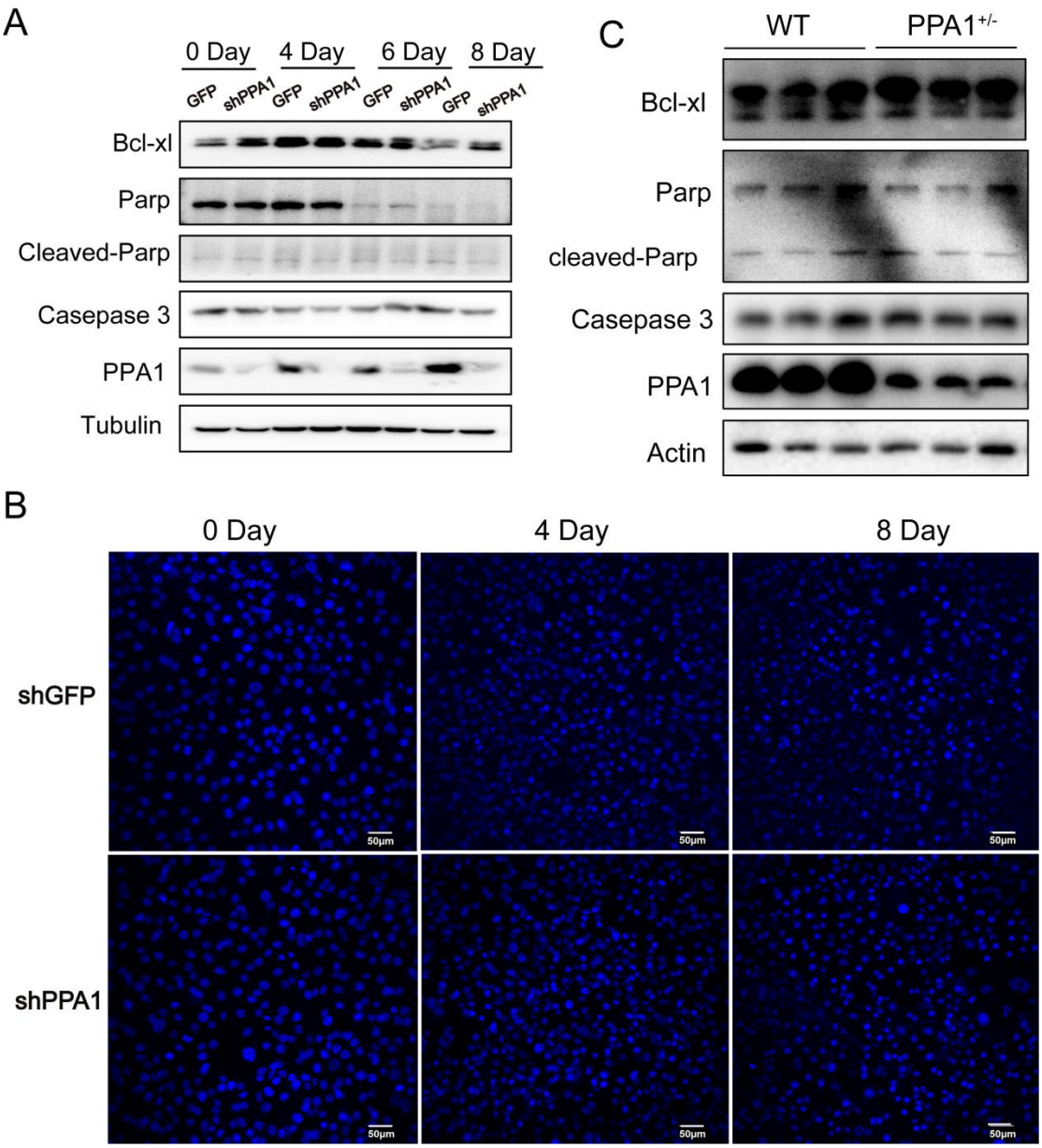

Supplementary Figure 7. Effect of PPA1 on cell apoptosis. A,B. 3T3-L1 preadipocytes were infected with lentiviral vector expressing control (shGFP) or PPA1 knockdown (shPPA1) shRNAs, cells were induced differentiation 2 days later and collected at indicated days. Apoptosis related gene expression was detected by Western blot (A) and cells were stained by Hoechst dye (B). Scale Bar=50 μm. C. Apoptosis related gene expression was detected in adipose tissue from WT and PPA1$^{+/-}$ mice by Western blot.

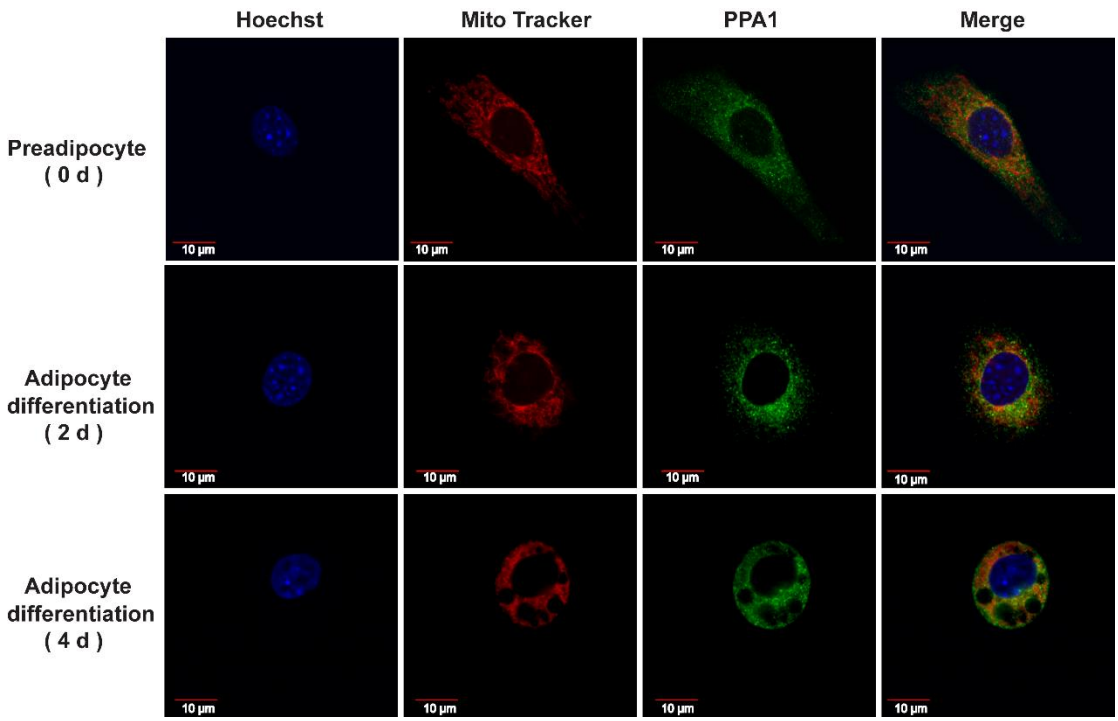

Supplementary Figure 8. Localization of PPA1 in 3T3-L1 cells during cell differentiation. Confocal imaging of 3T3-L1 cells stained with an antibody against PPA1 and with MitoTracker Red CMXRos (MTR). Individual images were merged digitally (Merge).

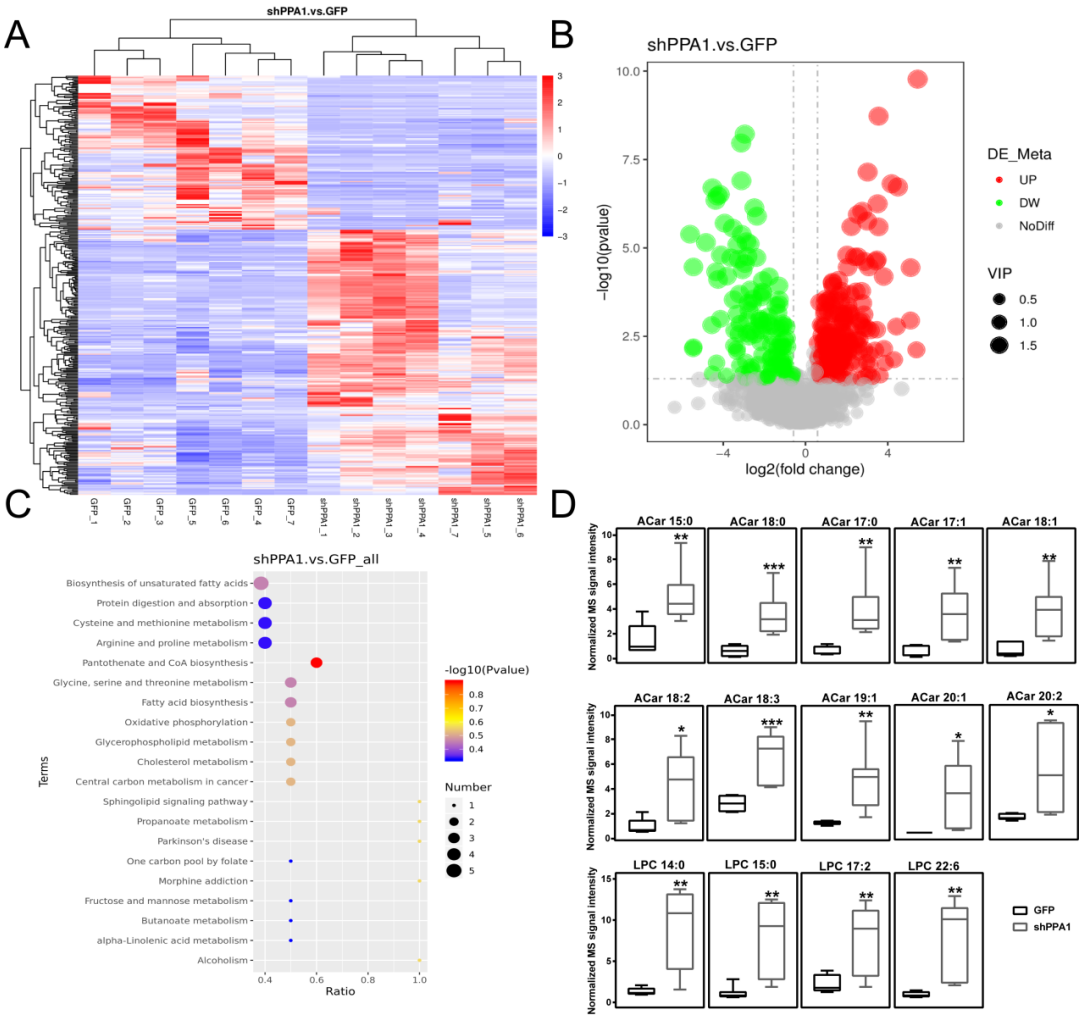

Supplementary Figure 9. Effect of PPA1 interference on adipocyte metabolome. SVF cells isolated from 4-week-old mice were infected with lentiviral vector expressing control (GFP) or PPA1 knockdown (shPPA1) shRNAs, cells were induced differentiation 2 days later and collected at Day 6. A. Hierarchical clustering of significantly different metabolites in cell lysate from control (GFP) and PPA1 deletion (shPPA1) adipocytes. Signal intensities were clustered in two dimensions (horizontal: metabolites; vertical: samples) on the basis of Euclidean distance. Colors indicate metabolite abundance as high (red), median (white), or low (blue). B. Volcano plot showing the difference in metabolites between GFP and shPPA1 group. C. KEGG enrichment analysis performed on the differentially expressed metabolites between

GFP and shPPA1 group. D. Values of specific metabolites are normalized to the median and expressed as box-and-whisker plots; n=7; *p<0.05, **p<0.01, ***p<0.001 compared with GFP.

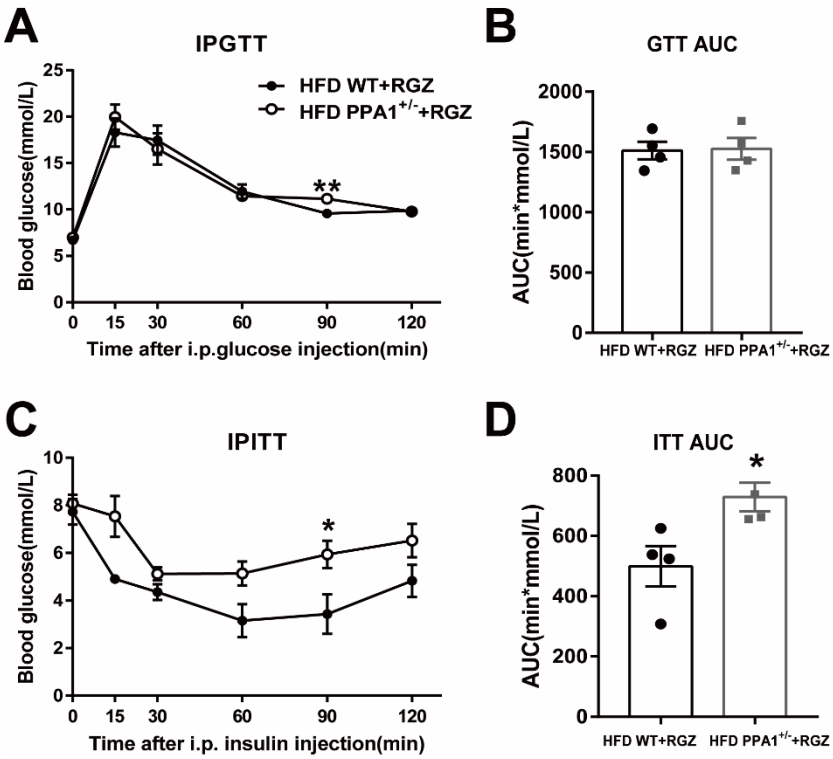

Supplementary Figure 10. Male 4-week-old PPA1$^{+/-}$ mice and WT littermates were fed with HFD for 12 weeks. Then mice were administrated with Rosiglitazone (5 mg/kg) by oral gavage for 10 days. GTT (A) and ITT (C) was performed and the area under curve was calculated (B,D). Data are represented as mean±SEM. *p<0.05, **p<0.01 compared with WT mice.

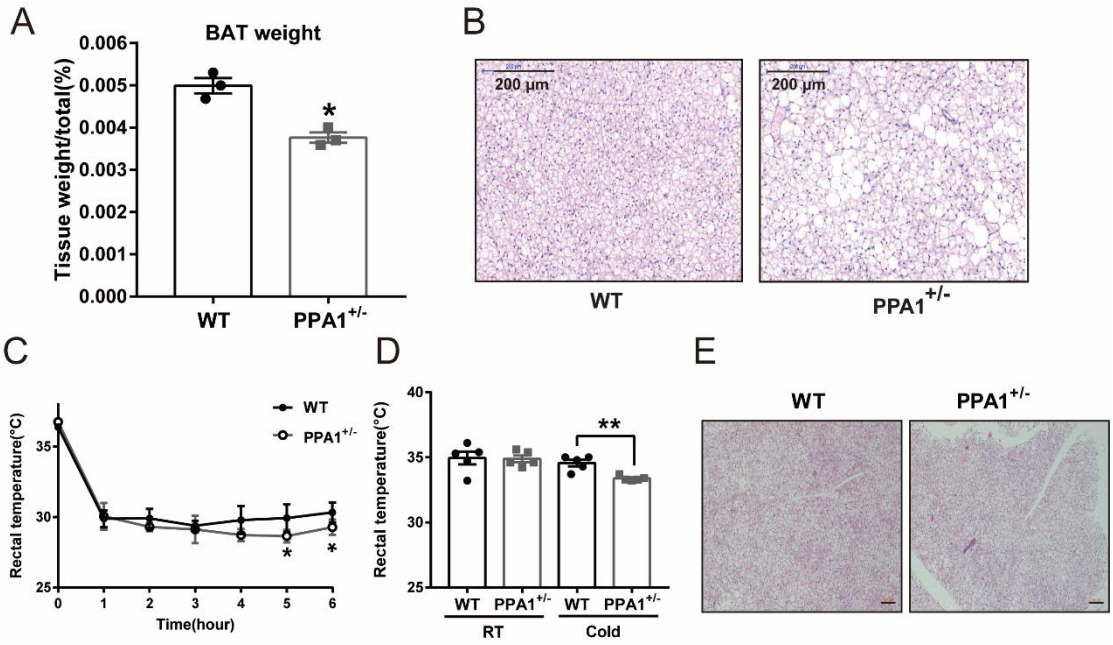

Supplementary Figure 11. HFD-fed PPA1$^{+/-}$ mice show decreased BAT mass and increased lipid accumulation. (A) BAT weight; (B) Representative images of H&E staining of BAT sections. Scale bar = 200 μm. C,D. Rectal temperature was monitored every hour for 6 h after exposure to a cold (4℃) environment. E. HFD-fed WT and PPA1$^{+/-}$ littermates were housed for 8 weeks at thermoneutrality (30℃). H&E staining of BAT from WT and PPA1$^{+/-}$ mice. Scale bar=100 μm. Data are represented as mean±SEM. *p<0.05, **p<0.01 compared with WT mice.